Isolation and Structure Elucidation of Chlorofusin, a Novel p53-MDM2 Antagonist from a *Fusarium* sp.

Sara J. Duncan, Sabine Grüschow, Dudley H. Williams,* Carole McNicholas,† Ravinder Purewal,† Michaela Hajek,† Martin Gerlitz,‡ Steven Martin,‡ Stephen K. Wrigley,‡ and Michael Moore†

Contribution from the Cambridge Centre for Molecular Recognition, University Chemical Laboratory, Lensfield Road, Cambridge CB2 1EW, U.K.

Received August 7, 2000

Abstract: Wild-type p53 plays a crucial role in the prevention of cancer. Since dysfunction of p53 can be caused by increased levels of the protein MDM2, small molecules which antagonize the interaction between these two proteins have potential in cancer therapy. The discovery and structure determination of a fungal metabolite, chlorofusin, which antagonizes the p53/MDM2 interaction are reported.

Introduction

The 53 kDa phosphoprotein p53 plays a critical role in the regulation of cell proliferation and controls cell growth and development of genetic abnormalities by inducing G1 arrest or apoptosis in response to DNA damage.[1] Dysfunction of p53, for example, by mutation of one of the well-known mutational hot spots of p53, is frequently associated with the development of cancers, and 50% of all human tumors are found to contain a mutated form of this gene.[2] p53 interacts closely with several viral and cellular proteins including the product of oncogene *Mdm2*, with which it forms a stable complex.[3,4] In this bound state, MDM2 conceals the DNA-binding domain of p53 so that it is unable to activate transcription of the genes needed for induction of G1 arrest or apoptosis.[5] p53 regulates the expression of *Mdm2* at the transcriptional level, creating an autoregulatory feedback loop for the *Mdm2* gene,[6] thus keeping the activity of p53 and levels of MDM2 in a cell in balance. Factors that act to increase the levels or activity of MDM2 disturb this balance, thereby promoting cell proliferation. When overexpressed, MDM2 therefore acquires tumorigenic potential.[7−9] The crystal structure of the MDM2−p53 complex has been determined, revealing three hydrophobic and aromatic p53 amino acids that make contacts within a hydrophobic cleft of MDM2.[10] These three side chains amount to approximately 300 Da, suggesting that the MDM2 pocket may be a suitable binding site for small molecules. It therefore seems possible that tumors expressing abnormally high levels of MDM2 could be treated by means of small molecules that disrupt the interaction between p53 and MDM2, thereby restoring normal function to p53.

A novel fungal metabolite has been identified as a result of a screening program which involved testing over 53 000 microbial extracts for the presence of inhibitors of the binding of p53 to MDM2. These extracts were generated from fermentations of a diverse collection of microorganisms including streptomycetes and other actinomycete bacteria and fungi representing a range of taxonomic orders and isolated from a wide variety of habitats.[11] We report the structure determination of this fungal metabolite, which antagonizes the p53/MDM2 interaction at the micromolar level, and which therefore has potential as a lead in cancer therapy. This novel peptide, which we have named chlorofusin, is an orange solid derived from fermentation of a microfungus assigned to the genus *Fusarium*. The experimental details of the production, isolation, and structure determination, which use established methods, are reported in detail in the Supporting Information.

Results

A. Taxonomy of the Producing Organism. In culture, strain 22026 produced a hyphomycete state assignable to the widespread genus *Fusarium*. Morphological studies revealed affinities with a number of species, including *Fusarium coccidicola* and *Fusarium ciliatum*, but a complete determination could not be secured with confidence.

B. Molecular Formula. The ESI mass spectrum of chlorofusin shows abundant $[MH]^+$ and $[MNa]^+$ ions at $m/z = 1363.7$ and 1385.7 Da, respectively, with a lower abundance $[MH_2]^{2+}$ ion at $m/z = 682.4$ Da. The accurate mass for the $[MH]^+$ ion has been determined by ESI FT/ICR spectroscopy as 1363.7016 Da. The isotope pattern indicates the presence of one chlorine atom, so the possible molecular formulas within 10 ppm of the accurate mass (Table 1) were generated by Xmass for the

† Xenova Ltd., 240 Bath Rd., Slough, Berkshire SL1 4EF, U.K.
‡ TerraGen Discovery (UK) Ltd., 545 Ipswich Rd., Slough, Berkshire SL1 4EQ, U.K.

(1) Haffner, R.; Oren, M. *Curr. Opin. Genet. Dev.* **1995**, *5*, 84−90.
(2) Levine, A. J.; Momand, J.; Finlay, C. A. *Nature* **1991**, *351*, 453−456.
(3) Momand, J.; Zambetti, G. P.; Olson, D. C.; George, D.; Levine, A. J. *Cell* **1992**, *69*, 1237−1245.
(4) Blommers, M. J. J.; Fendrich, G.; Garcia-Echeverria, C.; Chene, P. *J. Am. Chem. Soc.* **1997**, *119*, 3425−3426.
(5) Oliner, J. D.; Pietenpol, J. A.; Thiagalingam, S.; Gyuris, J.; Kinzler, K. W.; Vogelstein, B. *Nature* **1993**, *362*, 857−860.
(6) Wu, X.; Bayle, J. H.; Olson, D.; Levine, A. J. *Genes Dev.* **1993**, *7*, 1126−1132.
(7) Brown, D. R.; Thomas, C. A.; Deb, S. P. *EMBO J.* **1998**, *17*, 2513−2525.
(8) Fakharzadeh, S. S.; Trusko, S. P.; George, D. L. *EMBO J.* **1991**, *10*, 1565−1569.
(9) Capoulade, C.; Paillerets, B. B.-d.; Lefrere, I.; Ronsin, M.; Feunteun, J.; Tursz, T.; Wiels, J. *Oncogene* **1998**, *16*, 1603−1610.
(10) Kussie, P. H.; Gorina, S.; Marechal, V.; Elenbaas, B.; Moreau, J.; Levine, A. J.; Pavletich, N. P. *Science* **1996**, *274*, 948−953.
(11) Wrigley, S.; Hayes, M.; Thomas, R.; Chrystal, E. *Phytochemical Diversity: a Source of New Industrial Products*; RSC: Cambridge, 1997.

10.1021/ja002940p CCC: $20.00
Published on Web 01/09/2001

Table 1. Possible Molecular Formulas of Chlorofusin, Determined from the Accurate Mass

molecular formula	exact mass $[MH]^+$	error from measd mass (ppm)	molecular formula	exact mass $[MH]^+$	error from measd mass (ppm)
$C_{62}H_{99}O_{18}N_{14}Cl$	1363.7028	0.9	$C_{64}H_{103}O_{16}N_{12}ClS$	1363.7102	6.3
$C_{63}H_{95}O_{14}N_{18}Cl$	1363.7041	1.8	$C_{64}H_{95}O_{15}N_{16}Cl$	1363.6929	6.4
$C_{61}H_{99}O_{15}N_{16}ClS$	1363.6963	3.9	$C_{63}H_{99}O_{19}N_{12}Cl$	1363.6916	7.3
$C_{60}H_{99}O_{14}N_{18}ClS$	1363.7075	4.3	$C_{61}H_{99}O_{17}N_{16}Cl$	1363.7140	9.1
$C_{60}H_{103}O_{19}N_{12}ClS$	1363.6949	4.9	$C_{62}H_{95}O_{13}N_{20}Cl$	1363.7154	10.1

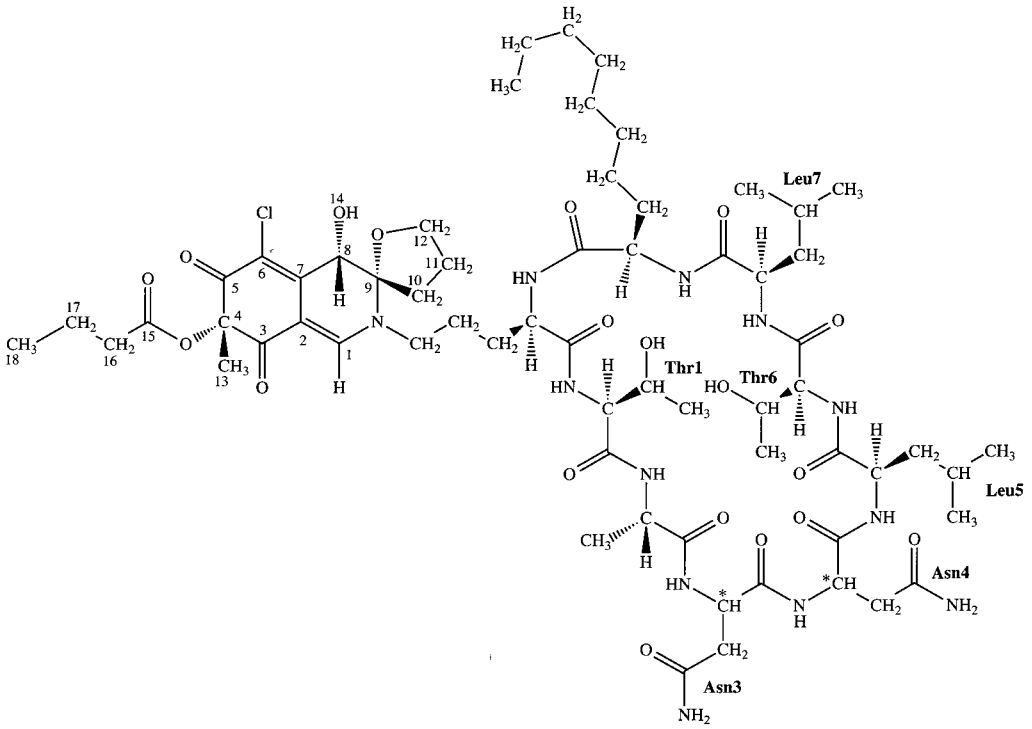

Figure 1. Proposed structure of chlorofusin. The absolute stereochemistries for C-4, C-8, and C-9 may be as shown, or with all three inverted. The two asparagine α-carbons marked with an asterisk have opposite stereochemistries; one is *R* and one is *S*.

following constraints: C_{60-64}, H_{80-110}, O_{12-20}, N_{12-20}, Cl_1, S_{0-1}. The formula was identified as $C_{63}H_{99}O_{19}N_{12}Cl$, on the basis of this mass determination (calcd 1363.6916 Da for the protonated species containing the ^{35}Cl isotope), the numbers of protons and carbons as seen in the ^1H and ^{13}C NMR spectra, the number of OH and amide NH groups (identified from the number of exchangeable protons), and the number of carbonyl oxygens, determined from the carbonyl region of the ^{13}C NMR spectrum.

C. Amino Acid Analysis. Amino acid analysis identified the following components: two leucines, two asparagine or aspartic acid residues, one alanine, two threonines, and the possibility of one or two nonstandard amino acids.

D. Functional Group Tests. Attempted acetylation of chlorofusin with acetic anhydride under aqueous conditions at pH 8.5 resulted in no change in the molecular mass (as determined by ESI TOF mass spectrometry), indicating the absence of basic amino groups. In contrast, acetylation with acetic anhydride in pyridine led to an increase in molecular mass of 126 Da, indicating the addition of three acetyl groups. It is therefore concluded that chlorofusin contains three hydroxyl functions which can be of a primary or secondary nature. The test for carboxylic acid functions with acidic methanol also proved negative as there was no mass increase of 14 Da observed for the molecular ion in the ESI mass spectrum. However, there was a mass increase of 15 Da that could be due to the rearrangement of one of the asparagine side chains to form isoaspartic acid, and the subsequent methylation of the resulting carboxylic acid. The UV absorption spectrum (methanol solution) showed λ_{max} (ϵ) 402 (12 870), 346 (9888), 202 (28 915). No changes were observed on acidification or basification. This observation indicates the presence of a strongly absorbing, conjugated chromophore.

E. NMR Spectroscopy. The structure of chlorofusin (Figure 1) was predominantly determined by NMR spectroscopy, using ^1H, ^{13}C, DEPT, DQF-COSY, TOCSY, NOESY, ROESY, $^1H-^{13}C$ HMQC, and $^1H-^{13}C$ HMBC experiments. The assigned proton and carbon resonances of chlorofusin in d_6-DMSO at 300 K are summarized in Table 2.

1. Assignment of the Amino Acids. The scalar coupling networks observed in the COSY and TOCSY spectra revealed fourteen characteristic spin systems, corresponding to two leucines, two threonines, alanine, a propyl chain, a five-membered ring, two amino groups, a C*H* (4.53 ppm) coupled to an adjacent O*H* (6.26 ppm), and four other amino acid fragments. The HMBC spectrum identified one of these four unknown amino acids as an asparagine residue by linking the β-CH_2 protons (2.48 and 2.75 ppm) and the NH_2 protons (7.00 and 7.24 ppm) through a common carbonyl carbon (170.3 ppm). The N*H* protons of the other amino group (resonances at 6.82 and 6.90 ppm) did not show any HMBC correlations, but it has been assumed to be linked to the unspecified amino acid with the equivalent β-CH_2 double doublet splitting pattern via a carbonyl group to form a second asparagine, thus satisfying the amino acid analysis data. The large integral for the protons

Table 2. Assignment of the ^{13}C and ^{1}H NMR Spectra of Chlorofusin

Assignment of the Amino Acid Macrocycle

residue	position	^{13}C chemical shift (ppm)	^{1}H chemical shift (ppm)	residue	position	^{13}C chemical shift (ppm)	^{1}H chemical shift (ppm)
Thr1	NH		8.73 (br s)	Thr6	NH		7.07 (br s)
	α-CH	63.1	3.66 (br s)		α-CH	62.1	3.92 (m)
	β-CH	65.0	4.02 (m)		*β*-CH	64.9	3.92 (m)
	γ-CH_3	20.3	1.16 (d)		*γ*-CH_3	20.2	1.10 (d)
	OH		5.28 (br s)		OH		5.05 (br s)
	α-carbonyl	173.0			α-carbonyl	170−174	
Ala2	NH		8.61 (d)	Leu7	NH		9.08 (br s)
	α-CH	50.8	3.95 (m)		α-CH	52.7	3.95 (m)
	β-CH_3	16.5	1.26 (m)		*β*-CH_2	38.7	1.60 (m)
	α-carbonyl	171.6			*γ*-CH	24.1	1.71−1.88 (m)
Asn3	NH		6.93 (br s)		*δ*-$CH_3 \times 2$	23.1 and 20.1	0.92 (d) and 0.82 (d)
	α-CH	49.0	4.75 (dt)		α-carbonyl	172.4	
	β-CH_2	37.3	2.62 (dd) and 2.93 (dd)	ADA8	NH		7.70 (d)
	γ-carbonyl	170−174			α-CH	53.9	4.02 (m)
	δ-NH_2		6.90 (br s) and 6.82 (br s)		*β*-CH_2	30.0	1.71−1.88 (m)
	α-carbonyl	170.9			*γ*-CH_2	25.9	1.26 (br m) and 1.38 (m)
Asn4	NH		7.84 (br s)		*δ*-CH_2	28.6	1.26 (br m)
	α-CH	52.0	4.41 (ddd)		*ϵ*-CH_2	28.5	1.26 (br m)
	β-CH_2	36.2	2.48 (dd) and 2.75 (dd)		*ζ*-CH_2	28.4	1.26 (br m)
	γ-carbonyl	170.3			*η*-CH_2	31.2	1.26 (br m)
	δ-NH_2		7.00 (br s) and 7.24 (br s)		*θ*-CH_2	22.0	1.26 (br m)
	α-carbonyl	170−174			*ι*-CH_3	13.9	0.87 (t)
Leu5	NH		7.51 (d)		α-carbonyl	171.9	
	α-CH	49.2	4.48 (dt)	Orn9	NH		6.69 (br s)
	β-CH_2	38.7	1.13 (br m) and 1.60 (m)		α-CH	51.2	4.59 (br t)
	γ-CH	24.0	1.41 (m)		*β*-CH_2	28.3	1.71−1.88 (m)
	δ-$CH_3 \times 2$	20.6 and 23.2	0.77 (d) and 0.78 (d)		*γ*-CH_2	27.0	1.71−1.88 (m) and 1.55 (sextet)
	α-carbonyl	173.1			*δ*-CH_2	50.5	3.42 (t)
					α-carbonyl	170−174	

Assignment of the Chromophoric Unit

position	^{13}C chemical shift (ppm)	^{1}H chemical shift (ppm)	position	^{13}C chemical shift (ppm)	^{1}H chemical shift (ppm)
1	150.0	7.77 (s)	10	30.3	2.38 (br m)
2	115.2		11	25.1	2.0−2.2 (m)
3	188.1		12	68.4	3.78 (q) and 4.02 (m)
4	84.7		13	22.9	1.43 (s)
5	188.7		14		6.26 (d)
6	101.3		15	171.4	
7	147.5		16	34.4	2.34 (t)
8	68.4	4.53 (d)	17	17.9	1.55 (sextet)
9	96.7		18	13.2	0.92 (t)

which resonate as a broad peak at 1.26 ppm implies the presence of a long chain of CH_2 groups which show couplings to both the methyl group at 0.87 ppm and the *β*-CH_2 protons (1.71−1.88 ppm) of one of the two remaining unassigned amino acids. This integral amounts to fourteen protons, three of which are in the side chain of alanine. Therefore, six CH_2 groups (five with both proton resonances at 1.26 ppm and one with protons at 1.26 and 1.38 ppm) were attached to the *β*-CH_2 group with proton resonances between 1.71 and 1.88 ppm. The methyl group (0.83 ppm) was then connected to the end of the chain. This forms an unusual amino acid, aminodecanoic acid, which has indeed been detected and identified by the EI mass spectrum in the GC−MS data. The final amino acid fragment from the COSY and TOCSY spectra has *β*-, *γ*-, and *δ*-CH_2 groups in the side chain, but it is not possible to determine any further connectivity from homonuclear couplings alone.

2. Interresidue Heteronuclear Correlations. HMQC and DEPT spectra were used to assign the carbon signals, and HMBC allowed some further connectivity to be determined, although very few cross-peaks were observed in the carbonyl/α-C*H* region. It was therefore only possible to determine two connections between the amino acid residues from the HMBC data. These connections were between the two asparagines, which showed a correlation from the carbonyl carbon at 170.9 ppm to both the α-C*H* of Asn4 and the *β*-CH_2 protons of Asn3, and between a leucine and the 2-aminodecanoic acid residues, which showed correlations from the carbonyl carbon at 172.4 ppm to the N*H* of 2-aminodecanoic acid and the α-C*H* and *β*-CH_2 protons of Leu7.

3. Assignment of the Chromophore. The structure of the chromophore proved more difficult to determine, but the large number of HMBC cross-peaks to the C*H* proton at position 1 significantly reduced the number of possibilities. The ^{13}C chemical shift of C-1 (150.0 ppm) suggests that it is both sp^2-hybridized and adjacent to an electronegative heteroatom. The HMBC spectrum shows six long-range correlations from this proton on C-1. Such correlations are typically found between protons and carbons that are separated by two or three bonds, but exceptionally occur through four bonds where these bonds are related in a W-pathway. On the basis of chemical shifts, the long-range couplings occurring from the proton on C-1 are to three quaternary carbons of C═C double bonds, to one carbonyl carbon, and to two sp^3-hybridized carbons (one quaternary and one methylene carbon). These sp^3-hybridized carbons have chemical shifts of 96.7 and 50.5 ppm, respectively. The former shift is characteristic of an sp^3-hybridized carbon

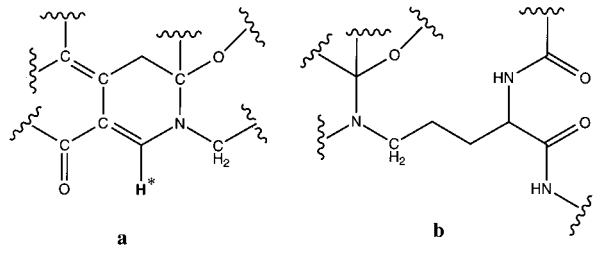

Figure 2. Structural elements of the chromophore.

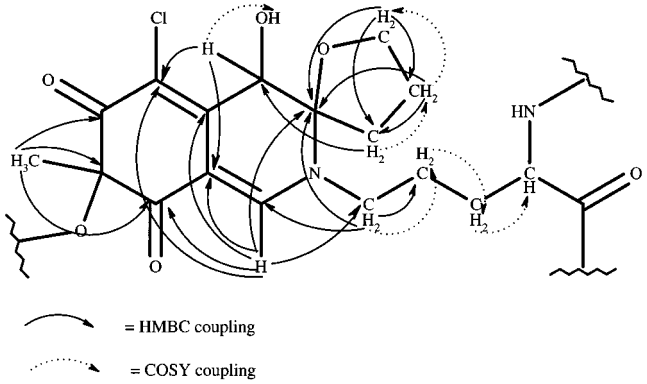

Figure 3. HMBC and COSY couplings in the chromophore.

attached to two electronegative atoms, and the latter is characteristic of an sp^3-hybridized carbon attached to one electronegative atom. These findings can be accommodated by the structural element of Figure 2a, where the asterisked proton is the singlet resonance that shows six HMBC couplings (to the carbons indicated by the symbol "C"). The CH_2 unit that is explicitly indicated in Figure 2a belongs to one of the fourteen spin systems described above, so it is further connected to be part of the structural unit shown in Figure 2b. It follows from the structural conclusions presented in Figure 2 that a forcing acid hydrolysis of chlorofusin should produce ornithine. This prediction has been confirmed, and the ornithine isolated from such hydrolysis has been shown to have the L absolute configuration (see later text for details). HMBC and COSY couplings to the other protons and carbons were used to construct the remainder of the chromophore (Figure 3).

F. Primary Structure. Connectivity between the remaining fragments has been resolved from the NOESY spectrum (mixing time 50 ms), using in particular the dipolar couplings between the α-C*H* of one amino acid and the N*H* of the adjacent residue. The sequential NOE correlations are shown in Figure 4; the long-range NOEs and those within R groups have been omitted for clarity. A ROESY experiment (mixing time 80 ms) confirmed that the observed NOEs between amide protons are indeed due to the nuclear Overhauser effect rather than exchange. This resulting structure (Figure 1) is the only possible arrangement of the amino acids in which there is an NOE correlation between the N*H* and adjacent α-C*H* protons of each residue, strongly supporting this structure as the correct sequence. There are no observed NOEs from the propyl group, suggesting that it is located away from the macrocyclic ring. The proposed ester linkage between the propyl group and the chromophore is in accord with this lack of NOEs as well as the mass spectrometry data. Upon MS−MS of the parent ion, the mass spectrum shows a peak at 1293.9 Da corresponding to a loss of 70 mass units, due to cleavage of the ester bond and proton transfer from the propyl chain to the ester oxygen (Scheme 1). Further evidence for this fragmentation comes from the mass spectrum acquired following the reaction of chlorofusin with pyridine and acetic anhydride. As described in the Functional Group Tests, there is a peak at $m/z = 1489.7$ in the mass spectrum, corresponding to an addition of 126 Da (three acetyl groups) to the molecular ion. There is also a peak at $m/z = 1461.7$ Da, which is an addition of 168 mass units to the ion corresponding to the loss of the propyl group (1293.9 Da), indicating the addition of four acetyl groups to the fragmented ion. Thus, during the reaction, the ester bond appears to have been cleaved, resulting in the formation of an extra hydroxyl group which is subsequently acetylated in addition to the three other hydroxyl functions. The MS−MS spectrum also shows an abundant singly charged ion at $m/z = 994.7$, corresponding to the loss of the entire chromophore (Scheme 2). This further supports the proposed structure, which excludes the chromophore from the macrocycle.

G. Stereochemistry. Chlorofusin was hydrolyzed (6 M HCl, 80 °C, 24 h), and the constituent amino acids were derivatized as the *N*,*O*-trifluoroacetylisopropyl esters for analysis by chiral gas chromatography. The amino acids were identified by comparison of the retention times with standards and by their EI mass spectra. By spiking the peptide with derivatives of the standard amino acids, the peptide peaks were found to correspond to L-alanine, D-asparagine, L-asparagine, 2 × D-leucine, 2 × L-threonine, and D-2-aminodecanoic acid (ADA). The peptide was hydrolyzed under stronger conditions (12 M HCl, 80 °C, 24 h) in attempt to identify the ornithine residue, which was then detected and identified as L-ornithine. The relative stereochemistry of the three chiral centers in the chromophore was determined by 1D gradient NOE experiments (DPFGSE NOE)[12] with variable mixing time to establish which NOEs had the fastest build-up rates. Upon irradiation of the proton attached to C-8 (4.53 ppm), negative NOEs were observed to the protons attached to both C-10 (2.38 ppm) and C-12 (3.78 ppm only) at a mixing time of 50 ms. With a shorter mixing time of 25 ms, only the NOE to the proton at C-10 was seen, enabling us to conclude that H-8 is closer to the protons on C-10 than those on C-12. Upon irradiation of the protons (1.43 ppm) of the quaternary methyl group attached to C-4, a single, weak NOE to the olefinic proton at 7.73 ppm was observed with a mixing time of 200 ms. The mixing time was increased to 500 ms, resulting in a negative NOE to H-8, but not to the hydroxyl proton 14. It can therefore be concluded that the protons attached to C-8, C-10, and C-13 all lie on the same side of the chromophore. One of the two possibilities is indicated in Figure 1, with the stereochemical ambiguities being indicated in the figure caption.

H. Secondary Structure. The remaining NOEs from the NOESY spectrum, together with deuterium exchange and variable temperature experiments, have provided information on the secondary structure of chlorofusin. Long-range NOEs build up between the following protons: Ala2 N*H* ↔ Orn9 β-CH_2 + γ-CH_2, Ala2 N*H* ↔ Orn9 α-C*H*, Leu5 N*H* ↔ Thr1 α-C*H*, Leu5 γ-C*H* ↔ Thr1 α-C*H*, Leu5 δ-CH_3 ↔ Thr1 α-C*H*, Leu5 δ-CH_3 ↔ Thr1 γ-CH_3, Leu5 δ-CH_3 ↔ ADA8 β-CH_2, Leu5 δ-CH_3 ↔ ADA8 $\gamma\rightarrow\theta$-CH_2, Thr6 N*H* ↔ Asn3 β-CH_2, Thr6 α-C*H* + β-C*H* ↔ Asn3 β-CH_2, Leu5 N*H* ↔ Asn3 N*H*, Thr1 α-C*H* ↔ Asn4 β-CH_2, Thr6 α-C*H* + β-C*H* ↔ ADA8 N*H*, and Thr6 N*H* ↔ Asn4 α-C*H*. To satisfy these correlations, the residues Leu5, Thr1, and ADA8 must all fold over the top of the macrocyclic ring of chlorofusin, while Asn3 folds underneath to reach the proximity of Thr6. For the Asn3 residue to fold in this way, it is likely that it has the L-configuration

(12) Stott, K.; Keeler, J.; Van, Q. N.; Shaka, A. J. *J. Magn. Reson.* **1997**, *125*, 302−324.

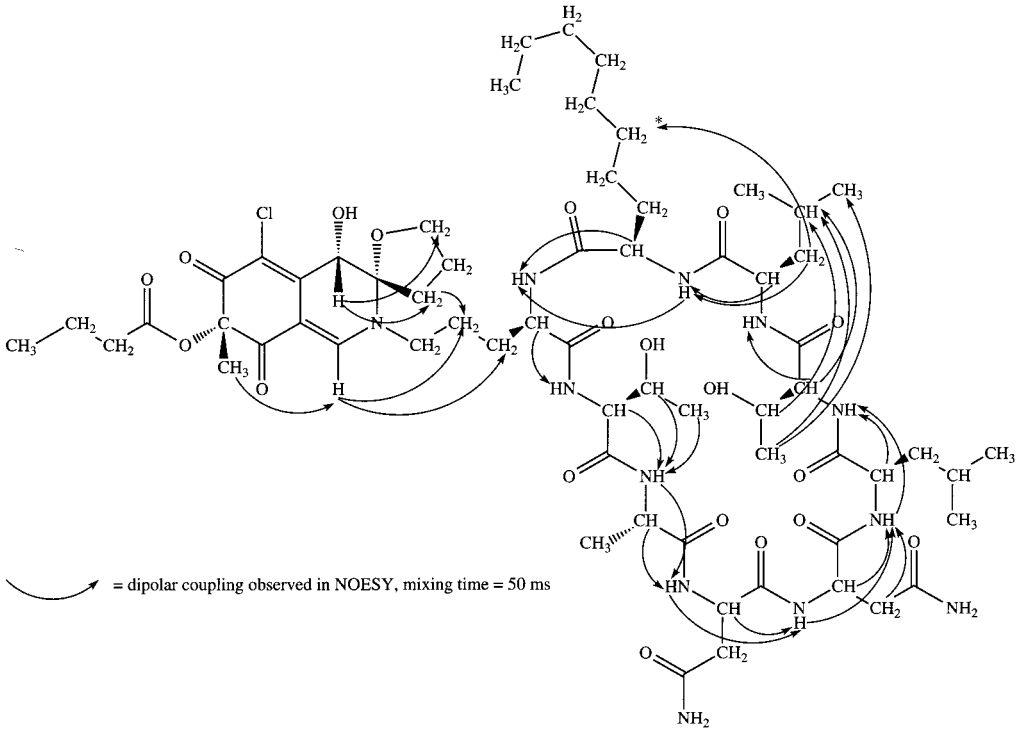

Figure 4. Sequential NOESY (mixing time 50 ms) correlations in chlorofusin. The asterisk indicates an NOE to part of the chain of ADA, but it is not possible to distinguish between these protons.

Scheme 1

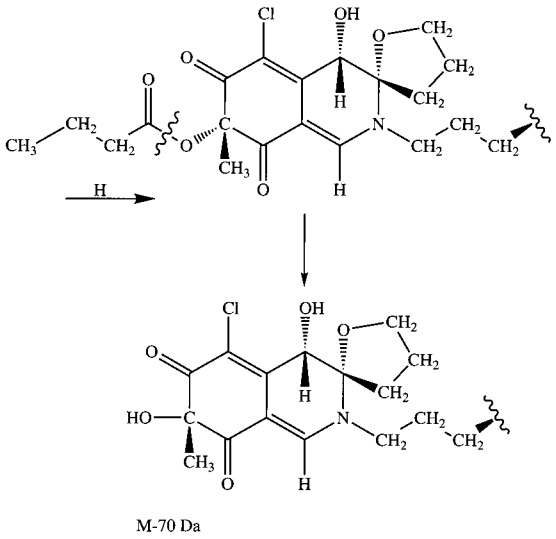

Scheme 2

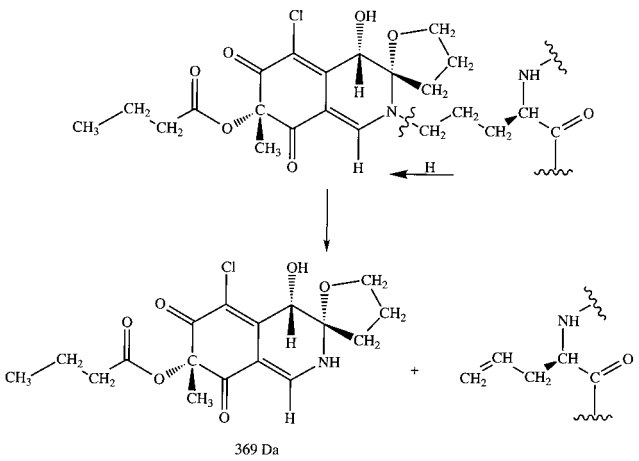

while Asn4 has the D absolute stereochemistry. Where possible, N*H*−α-C*H* coupling constants have been measured in the 1D spectrum to obtain conformational information, but with the exception of the amide resonances in Ala2 ($J = 3.2$ Hz), Leu5 ($J = 9.3$ Hz), and ADA8 ($J = 7.3$ Hz), the J couplings could not be resolved. In all cases except for Thr6, this lack of resolution was due to broad line shapes, but for Thr6, the narrow line width of the amide proton (7.9 Hz) puts an upper limit of approximately 4 Hz on the coupling constant. The modified Karplus curve[13] has been used to extract values of angle θ for the four residues with assigned coupling constants. Residues Ala2 and Leu5 have respective approximate θ values of 60° or 110°, and 160°or 170° (effectively trans). Thr6 has a range of possible values of θ between 50° and 120°, but the coupling constant value of 7.3 Hz for ADA8 does not give any conclusive information on the torsion angle. All these restraints have been incorporated into the 3D structure (see the Discussion). D_2O (5 vol %) was added to the NMR sample, and proton NMR spectra were recorded immediately after the shake and at subsequent 5 min intervals. (There was no further change in the spectra after the first spectrum following the addition of D_2O was acquired.) Where peaks were resolved, it was clear which ones exchanged quickly, and which ones kept their intensity. However, other peaks merged so that it was impossible to determine their rate of exchange. Additionally, the temperature coefficients of the amide protons were measured over the range 300−340 K. It is normally assumed that relatively high temperature coefficients (>3.5 ppb K^{-1}) indicate a high degree of solvent exposure. However, it was found that in some cases the two sets of results were contradictory. The results of both D_2O exchange and temperature dependence are shown in Table 3. In our interpretation of the data (see the Discussion), we assume that the best evidence for strong intramolecular hydrogen bonding is es-

(13) Wuthrich, K. *NMR of Proteins and Nucleic Acids*; John Wiley & Sons: New York, 1986.

Table 3. Deuterium Exchange Data and Temperature Coefficients for the Amide and Hydroxyl Protons

residue	resonance (ppm)	% integral of original peak after addition of 5% D_2O	shift over 40 K (ppm)	shift (ppb K^{-1})[a]	conclusion
Leu7	9.08	92	0.28	7	slow exchange
Thr1	8.73	100?[b]	0.35	8.75	
Ala2	8.61		0.42	10.5	
Asn4	7.84	52?[c]	0.08	2	
ADA8	7.70	96	0.05	1.25	slow exchange
Leu5	7.51	100	0.01	0.25	slow exchange
Asn4 δ-NH	7.24	33	0.15	3.75	fast exchange
Thr6	7.07	100	0.00	0	slow exchange
Asn4 δ-NH	7.00	17	0.23	5.75	fast exchange
Asn3	6.93	?[d]	0.03	0.75	
Asn3 δ-NH	6.90		0.18	4.5	
Asn3 δ-NH	6.82		0.03	0.75	
Orn9	6.69	100	0.12	3	slow exchange
chromophore 14	6.26	11	0.18	4.5	fast exchange
Thr1 OH	5.28	12	0.15	3.75	fast exchange
Thr6 OH	5.05	0	0.22	5.5	fast exchange

[a] $T_c > 3.5$ ppb K^{-1}, high solvent-exposed area; $T_c < 3.5$ ppb K^{-1}, low solvent-exposed area. [b] Upon addition of 5% D_2O, these two resonances and an impurity peak merged together so that it was impossible to measure the integrals accurately. [c] This peak moved downfield underneath the aromatic C*H* signal after addition of D_2O. [d] All three of these resonances merged together, making it impossible to distinguish between them.

sentially complete protection from D_2O exchange, i.e., the NH residues of Leu5, Thr6, Leu7, ADA8, and Orn9.

I. Biological Activity. Chlorofusin was one of the major components produced in fermentations of *Fusarium* sp. 22026. Several minor fermentation components were related to chlorofusin as they had identical UV−vis absorption spectra. The DELFIA-modified ELISA was used to guide the purification of inhibitors of the p53/MDM2 interaction from these fermentation extracts. Chlorofusin was the most abundant inhibitory compound, but two other active compounds related to chlorofusin were also isolated in small quantities, and the structures of these compounds will be reported subsequently. Titration of purified chlorofusin in the DELFIA-modified ELISA gave an IC_{50} of 4.6 μM. In simultaneous cross-screen testing, chlorofusin was inactive at a concentration of 4 μM in the TNFα:TNFα receptor protein−protein interaction, which was configured in the same format as the primary assay. The compound showed no cytotoxic effects against Hep G2 cells at a concentration of 4 μM. At a test concentration of 7.3 μM, chlorofusin did not exhibit any antimicrobial activity against the following test strains: *Escherichia coli* NCIMB 12210, *Staphylococcus aureus* ATCC 29213, *Serratia marcescens* NCIMB 8889, *Bacillus subtilis* NCIMB 8054, *Klebsiella pneumoniae* NCIMB 9111, *Proteus vulgaris* NCIMB 4175, *Candida albicans* NCPF 3121, *Cryptococcus neoformans* NCPF 3379, and *Aspergillus niger* NCPF 2190.

Discussion

A proposed model of the folded structure of chlorofusin based on the NMR data and the use of CPK models has residues ADA8, Leu5, and Thr1 folded on top of the ring as described above, forming a hydrophobic cluster on one face of the peptide. Residue 3 lies underneath the cycle to satisfy the observed NOEs to the Thr6 residue, and is possibly held by a hydrogen bond between the δ-N*H* of Asn3 at 6.82 ppm and the hydroxyl oxygen of Thr6. This would account for the low-temperature coefficient observed for this amide proton, and could also explain why a much broader peak is seen for the Thr6 O*H* (5.05 ppm) than the Thr1 O*H* (5.28 ppm). The presence of this hydrogen bond forces the β-CH_2 protons of Asn3 to be aligned so as to imply a π-contribution to the geminal coupling constant, i.e., $J_{gem} > 13$ Hz.[14] This is indeed the case ($J = 15.2$ Hz), thus supporting this proposed interaction. The results in Table 3 show that there are four amide protons (those on residues ADA8, Leu5, Thr6, and Orn 9) that are unambiguously in slow exchange (i.e., both the D_2O exchange and the temperature dependence experiments were in agreement), so these should be involved in intramolecular hydrogen bonds and/or be buried within the molecule. We hypothesize that chlorofusin has a β-turn motif involving a hydrogen bond between Orn9 N*H* and the carbonyl of Thr6, with an additional stabilizing hydrogen bond between the N*H* of Thr6 and the carbonyl of Orn9. A β-bulge[15] is also proposed to be formed by a hydrogen bond between Leu5 N*H* and the carbonyl of Thr1. These hydrogen bonds are not only in accord with well-known peptide folding patterns, but they also bring residues 1 and 5 into close proximity, thus satisfying many of the long-range NOEs. It is possible that ADA8 N*H* is hydrogen-bonded to part of the chromophore, but we do not have sufficient evidence to render this conclusion unambiguous as there are no NOESY or ROESY cross-peaks between the protons in the chromophore and protons in the macrocycle. The proposed structural elements are also in agreement with the measured N*H*−α-C*H* coupling constants. The β-bulge forces the alanine residue to have a α-CH−NH torsion angle of approximately 90°, which is consistent with the observed coupling constant of 3.2 Hz. Similarly, with this β-sheet-type structure, the equivalent torsion angle for Leu5 is 180°, which again is consistent with the coupling constant of 9.3 Hz. Those elements of the secondary structure in which we can have the highest confidence are depicted in Figure 5.

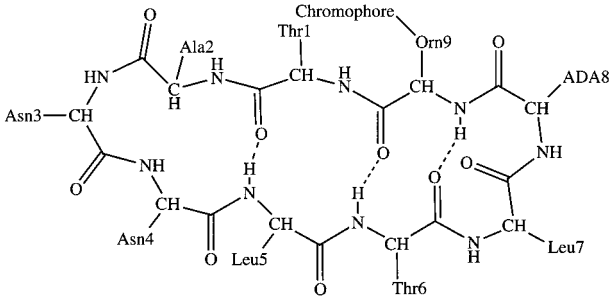

Figure 5. Proposed hydrogen bonding (dotted lines) in chlorofusin. Note: The Asn3 residue folds underneath the macrocyclic ring and is possibly hydrogen-bonded to the hydroxyl oxygen of Thr6.

(14) Bhacca, N. S.; Williams, D. H. *Applications of NMR Spectroscopy in Organic Chemistry*; Holden-Day, Inc., San Francisco, CA, 1964.

(15) Richardson, J. S.; Getzoff, E. D.; Richardson, D. C. *Proc. Natl. Acad. Sci. U.S.A.* **1978**, *75*, 2574−2578.

Conclusion

The primary structure of a fungal secondary metabolite has been elucidated by means of NMR, mass spectrometry, and chiral GC−MS. Some details of a secondary structure have been proposed on the basis of long-distance NOE correlations, amide proton exchange rates and temperature coefficients, and scalar coupling constants. The structure is one of a class of structurally similar compounds (unpublished work) which antagonize the interaction between p53 and MDM2, and is therefore of potential interest in cancer therapy.

Acknowledgment. We thank Dr. Martyn Ainsworth of TerraGen Discovery (UK) Ltd. and Prof. W. Gams (Centraalbureau voor Schimmelcultures, Baarn, The Netherlands) for taxonomic assistance, Dr. Leonard Packman for performing the amino acid analysis, the Medical Research Council for financial support to S.J.D., and the MRC Biomedical NMR Centre, Mill Hill, London, for access to their NMR facilities. The p53/MDM2 screening program was part of a discovery partnership between Xenova Ltd. and Genzyme Molecular Oncology, and was also supported by the NCI under the NPDDCG program.

Supporting Information Available: Experimental details (PDF). This material is available free of charge via the Internet at http://pubs.acs.org.

JA002940P